

Synthesis Design | Hot Paper |

Efficient Blue Phosphorescence in Gold(I)-Acetylide Functionalized Coinage Metal Bis(amidinate) Complexes

Thomas J. Feuerstein,^[a] Tim P. Seifert,^[a] André P. Jung,^[a] Rouven Müller,^[b] Sergei Lebedkin,^[c] Manfred M. Kappes,^[c, d] and Peter W. Roesky^{*[a]}

Abstract: The synthesis of linear symmetric ethynyl- and acetylide-amidinates of the coinage metals is presented. Starting with the desilylation of the complexes $[\{\text{Me}_3\text{SiC}\equiv\text{CC}(\text{NDipp})_2\}_2\text{M}_2]$ (Dipp = 2,6-diisopropylphenyl) (M = Cu, Au) it is demonstrated that this compound class is suitable to serve as a versatile metalloligand. Deprotonation with *n*-butyllithium and subsequent salt metathesis reactions yield symmetric tetranuclear gold(I) acetylide complexes of the form $[\{\{\text{PPh}_3\}\text{AuC}\equiv\text{CC}(\text{NDipp})_2\}_2\text{M}_2]$ (M = Cu, Au). The corresponding Ag complex $[\{\{\text{PPh}_3\}\text{AuC}\equiv\text{CC}(\text{NDipp})_2\}_2\text{Ag}_2]$ was ob-

tained by a different route via metal rearrangement. All compounds show bright blue or blue-green microsecond long phosphorescence in the solid state, hence their photophysical properties were thoroughly investigated in a temperature range of 20–295 K. Emission quantum yields of up to 41% at room temperature were determined. Furthermore, similar emissions with quantum yields of 15% were observed for the two most brightly luminescent complexes in thf solution.

Introduction

In the last decades, a great number of luminescent coinage metal complexes have been reported in the literature.^[1] The ligands applied for the synthesis of these complexes varied broadly from, for example, differently substituted phosphines,^[2] NHCs,^[3] to multidentate P,N-type^[4] ligands. Another ligand group are ethynyl or acetylide containing compounds,^[5] which are highly attractive for several reasons: 1) their ability to realize σ - and π -coordination modes allows for the synthesis of multinuclear complexes with short metal–metal contacts;^[6]

2) their multidentate character and linearity are key factors for the formation of supramolecular structures;^[7] 3) the $\text{C}\equiv\text{C}$ moiety is often involved in photophysical processes in organometallic compounds. The latter is related to *intra*ligand or *metal-to-ligand charge transfer* to the $\pi^*(\text{C}\equiv\text{C})$ orbitals upon photoexcitation, from which radiative relaxation can also occur.^[8] Concerning photoluminescence (PL) among coinage metal complexes, the phenomenon of metallophilicity often plays a significant role as well. Metallophilicity describes the tendency of metal cations to form very short metal–metal contacts, which occur mostly in the solid state.^[9] The metallophilic interactions may have a strong impact on the photophysical properties,^[10] however, the relations between the structure and the resulting properties are still a matter of investigations.^[11]

Dependent on the ligand, metallophilic interactions are classified into unsupported, semi-supported and fully supported ones.^[12] For example, monovalent coinage metal amidinate complexes are known to form dimeric species “ L_2M_2 ”, exhibiting fully supported metal–metal contacts that go along with metallophilic interactions.^[13] Therefore, those complexes may show distinct PL depending on the amidinate substituents.^[12,14] Our group recently reported on the alkynyl substituted gold(I) amidinate $[\{\text{Me}_3\text{SiC}\equiv\text{CC}(\text{NDipp})_2\}_2\text{Au}_2]$ with an inherent aurophilic interaction indicated by an extraordinarily short gold–gold contact (Au1–Au1' 2.7009(11) Å). Furthermore, this complex shows distinct PL in the solid state, as well as in tetrahydrofuran (thf). It has also been demonstrated that further reaction with $[\text{AuCl}(\text{tht})]$ (tht = tetrahydrothiophene) results in a desilylation, yielding an octanuclear species.^[15]

Herein, we describe a reaction protocol for the controlled desilylation of the $-\text{C}\equiv\text{C}-\text{SiMe}_3$ group to obtain the versatile luminescent building block $[\{\text{HC}\equiv\text{CC}(\text{NDipp})_2\}_2\text{Au}_2]$ for subse-

[a] Dr. T. J. Feuerstein, Dr. T. P. Seifert, A. P. Jung, Prof. Dr. P. W. Roesky
Institute of Inorganic Chemistry, Karlsruhe Institute of Technology (KIT)
Engesserstrasse 15, 76131 Karlsruhe (Germany)
E-mail: roesky@kit.edu

[b] Dr. R. Müller
Macromolecular Architectures, Institute for Chemical Technology and
Polymer Chemistry (ITCP), Karlsruhe Institute of Technology (KIT)
Engesserstrasse 18, 76131 Karlsruhe (Germany)

[c] Dr. S. Lebedkin, Prof. Dr. M. M. Kappes
Institute of Nanotechnology, Karlsruhe Institute of Technology (KIT)
Hermann-von-Helmholtz-Platz 1, 76344
Eggenstein-Leopoldshafen (Germany)

[d] Prof. Dr. M. M. Kappes
Institute of Physical Chemistry, Karlsruhe Institute of Technology (KIT)
Fritz-Haber Weg 2, 76131 Karlsruhe (Germany)

Supporting information and the ORCID identification number(s) for the author(s) of this article can be found under:
<https://doi.org/10.1002/chem.202002466>.

© 2020 The Authors. Published by Wiley-VCH GmbH. This is an open access article under the terms of Creative Commons Attribution NonCommercial License, which permits use, distribution and reproduction in any medium, provided the original work is properly cited and is not used for commercial purposes.

quent reactions such as lithiation with a strong base. The efficiency of this protocol is ascribed to the kinetic stabilization of the metal core by the bulky 2,6-diisopropylphenyl (Dipp) substituents. The controlled metalation of the ethynyl end group allows for the preparation of multinuclear complexes, which represent potential building blocks for the synthesis of heterometallic metalpolymers. In addition, the access is extended to the other coinage metals copper and silver. In this manner, small molecules with promising photophysical characteristics are obtained.^[16] Indeed, all complexes investigated in this work show bright blue or blue-green PL both in the solid state and in solution.

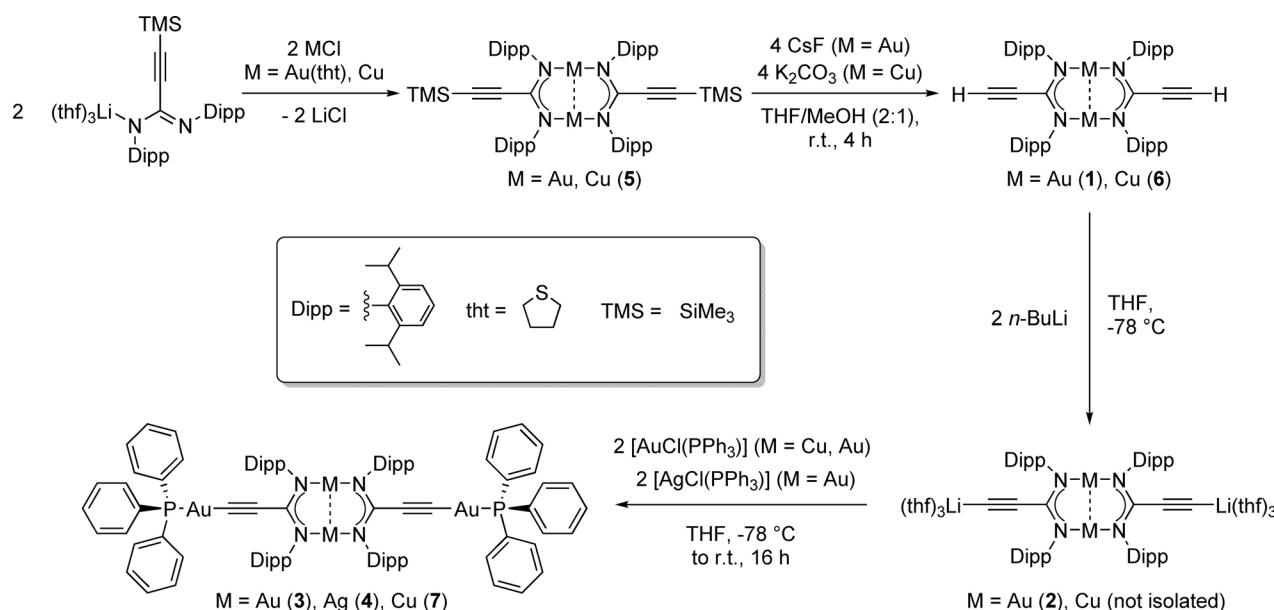
The efficient PL in solution might result from the structural motif with inherently short metal-metal contacts (metallophilic interactions), which are still existent even after the dimeric coinage metal amidinates are dissolved.^[15]

Results and Discussion

As starting point, the previously published compound $[(\text{Me}_3\text{SiCC}(\text{NDipp})_2)_2\text{Au}_2]$ was used,^[15] which was desilylated with caesium fluoride in a 2:1 stoichiometric mixture of absolute thf and methanol to yield the desired complex $[(\text{HC}\equiv\text{CC}(\text{NDipp})_2)_2\text{Au}_2]$ (**1**) in almost quantitative yield (Scheme 1). The desilylation towards compound **1** was initially verified by NMR measurements. In the ^1H NMR spectrum of **1**, no resonances were observed in the region for trimethylsilyl groups ($\delta \approx 0$ ppm), while the protons of the terminal alkynes were detected as a singlet resonance at $\delta = 2.64$ ppm. In the $^{13}\text{C}\{^1\text{H}\}$ NMR spectrum, the resonances for the alkyne moieties at $\delta = 89.1$ and 75.8 ppm are significantly shifted to lower ppm compared to the analogue resonances of the starting compound ($\delta = 109$ and 97.3 ppm). Furthermore, two characteristic bands for the stretching modes of the terminal alkyne at $\tilde{\nu}(\text{C}-\text{H}) = 3276\text{ cm}^{-1}$ and $\tilde{\nu}(\text{C}\equiv\text{C}) = 2114\text{ cm}^{-1}$ arise in the IR spectrum of

1. The latter is also observed as the signal with the highest intensity in the Raman spectrum of **1** at $\tilde{\nu}(\text{C}\equiv\text{C}) = 2113\text{ cm}^{-1}$. This mode is shifted by 53 cm^{-1} to smaller wavenumbers in comparison to the parent compound. The purity of compound **1** was confirmed via elemental analysis, as well as HR-ESI mass spectrometry. Thereby, the compound was detected in form of its molecule peak $[M]^+$ at $m/z = 1168.4932$.

The structural integrity of compound **1** in the solid state was finally verified by single crystal X-ray analysis (Figure 1). All bond lengths and angles are similar to the starting material, for example, the gold-gold distance ($\text{Au}-\text{Au}'$ $2.7055(5)\text{ \AA}$) as well as the carbon-carbon triple bond ($\text{C}2-\text{C}3$ $1.182(5)\text{ \AA}$) are nearly identical to the observed values for $[(\text{Me}_3\text{SiCC}(\text{NDipp})_2)_2\text{Au}_2]$ ($\text{Au}-\text{Au}'$ $2.7009(11)\text{ \AA}$ and $\text{C}2-\text{C}3$ $1.184(6)\text{ \AA}$). Compound **1** is a versatile precursor for the synthesis of multinuclear metal complexes because the terminal alkyne function can be further derivatized. Subsequently, the auration of the alkyne moiety by a one-pot reaction with KHMDS and $[\text{AuCl}(\text{PPh}_3)]$ was tested, but it was not possible to obtain the desired product. Therefore, a stepwise approach was chosen. In the first step, complex **1** was reacted with two equivalents of *n*-butyllithium at -78°C to yield the lithium acetylide $[(\text{thf})_3\text{LiCC}(\text{NDipp})_2)_2\text{Au}_2]$ (**2**) (Scheme 1). Interestingly, since compound **1** shows a cyan colored luminescence in solution, the deprotonation towards complex **2** can be easily monitored by the immediate change of the luminescence to azure after addition of the base, using a conventional UV-lamp ($\lambda_{\text{exc}} \approx 365\text{ nm}$). Full deprotonation of compound **1** was proved by the ^1H NMR spectrum of **2**, in which, in contrast to the spectrum of **1**, no resonances for the terminal alkyne protons were observed. Furthermore, all coordinating thf molecules can be eliminated by thoroughly drying of the product under reduced pressure. However, traces of non-deuterated thf are visible in the ^1H NMR spectrum. In the $^{13}\text{C}\{^1\text{H}\}$ NMR spectrum of **2**, the resonances for the alkyne moieties at $\delta = 123.7$ and 104.2 ppm



Scheme 1. Synthesis of compounds 1–7.

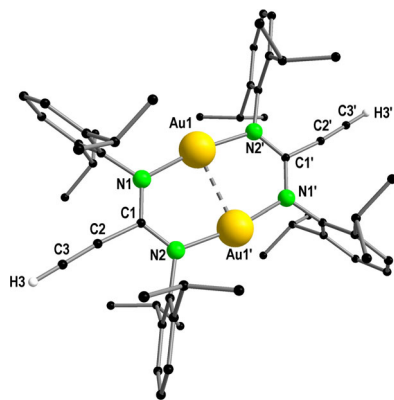


Figure 1. Molecular structure of compound **1** in the solid state. Hydrogen atoms, except for the terminal alkyne protons, are omitted for clarity. Structural parameters are given in the Supporting Information.

are clearly shifted to higher ppm in comparison to complex **1**, as well as to $[(\text{Me}_3\text{SiC}\equiv\text{CC}(\text{NDipp})_2)_2\text{Au}_2]$. In addition, a single resonance in the $^7\text{Li}\{^1\text{H}\}$ NMR spectrum of **2** is detected as a singlet at $\delta = -0.88$ ppm in the usual range for lithium acetylides.^[17]

The very intense stretching mode of the carbon–carbon triple bond in the Raman spectrum at $\tilde{\nu}(\text{C}\equiv\text{C}) = 2038\text{ cm}^{-1}$ is shifted by 75 cm^{-1} to smaller wavenumbers in comparison to **1**. As expected, compound **2** is highly moisture sensitive and immediately reacts back to **1** upon exposure to air, which can be easily observed by the aforementioned change in the emission color under irradiation with an UV-lamp. However, the compound is quite temperature stable and could be obtained in form of large needle shaped colorless crystals by recrystallization from thf. Single crystal X-ray diffraction revealed that the lithium atoms in compound **2** are coordinated tetrahedrally by three thf molecules and the acetylide carbon atom (Figure 2). The O–Li–C and O–Li–O bond angles in the range of $96.0(9)–119.0(10)^\circ$ are all close to the ideal tetrahedral angle of 109.5° .

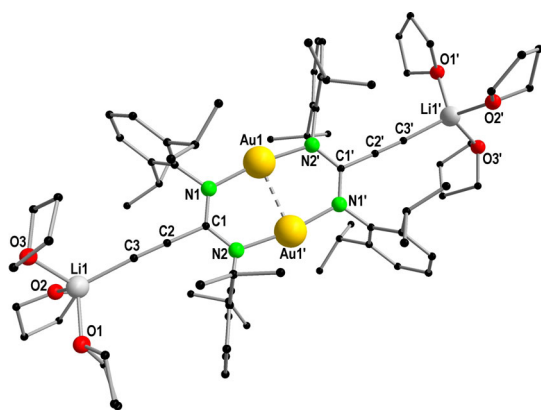


Figure 2. Molecular structure of compound **2** in the solid state. Hydrogen atoms are omitted for clarity. Structural parameters are given in the Supporting Information.

Quite unusually, no agglomeration of the lithium acetylide moieties is observed. In fact, there is no report of a crystallographically investigated compound with an isolated end-on Li–C coordination, so far. The C2–C3–Li1 angle of $175.6(7)^\circ$ is close to the ideal value of 180° for the end-on coordination. Nevertheless, the C3–Li1 distance of $2.06(2)\text{ \AA}$ is comparable to other lithium acetylides.^[18]

The structural parameters of the central gold-containing stretched hexagonal motif show no significant deviations in comparison to the molecular structure of compound **1**, for example, the gold–gold distance is in the same range (Au1–Au1' $2.6837(5)\text{ \AA}$). However, the carbon–carbon triple bond length C2–C3 of $1.219(10)\text{ \AA}$ is slightly longer than the determined values for the starting material **1**.

For the synthesis of the desired coinage metal functionalized compounds, the lithium acetylide **2** was reacted in salt metathesis reactions with coinage metal halides. First, the *in situ* generated complex **2** was reacted with two equivalents of chloro(triphenylphosphine)gold(I) to give the tetranuclear gold complex $[(\text{PPh}_3)_2\text{AuC}\equiv\text{CC}(\text{NDipp})_2)_2\text{Au}_2]$ (**3**) (Scheme 1). Recrystallization from dichloromethane/*n*-pentane resulted in a colorless microcrystalline solid. The ^1H NMR spectrum of **3** is comparable to the parent compound, except that the proton resonances of the triphenylphosphine moieties are observed as a separate multiplet in the range of $\delta = 7.52–7.34$ ppm. In comparison to compound **2**, the alkyne carbon resonances in the $^{13}\text{C}\{^1\text{H}\}$ NMR spectrum are detected at higher ppm values, i.e. at $\delta = 155.3$ and 123.7 ppm. Both resonances are detected as doublets with coupling constants of $^2J_{\text{CP}} = 145.9\text{ Hz}$ (Au–C) and $^3J_{\text{CP}} = 32.2\text{ Hz}$ (Au–C≡C), respectively. The phosphine resonance in the $^{31}\text{P}\{^1\text{H}\}$ NMR spectrum appears at $\delta = 41.2$ ppm and therefore at the usual chemical shift for Au(PPh₃) substituted alkynes.^[19] In the IR spectrum of compound **3**, a broad weak band is observed for the asymmetric combination of the C≡C stretching at $\tilde{\nu}(\text{C}\equiv\text{C}) = 2109\text{ cm}^{-1}$. The analogue symmetric combination is observed in the Raman spectrum at $\tilde{\nu}(\text{C}\equiv\text{C}) = 2117\text{ cm}^{-1}$ as the band with the highest intensity. Finally, single crystal X-ray diffraction revealed that the initially desired tetranuclear gold complex **3** was obtained (Figure 3, left). In analogy to the previously discussed compounds, the structural parameters for the central motif show no significant changes. The Au2 atom of the Au(PPh₃) fragment is linearly coordinated by the acetylide moiety. The C3–Au2–P1 angle of $173.5(2)^\circ$ is close to the ideal angle of 180° . The Au2–P1 distance of $2.272(2)\text{ \AA}$, as well as the Au2–C3 distance of $1.993(7)\text{ \AA}$, are comparable to similar compounds.^[20]

Consecutively, we felt challenged to synthesize the acetylides of the lighter congeners of gold. Therefore, two equivalents of chloro(triphenylphosphine)silver(I) were added to *in situ* generated compound **2**. After a similar workup as for the tetranuclear gold complex **3**, to our surprise, $[(\text{PPh}_3)_2\text{AuC}\equiv\text{CC}(\text{NDipp})_2)_2\text{Ag}_2]$ (**4**) was obtained as a white microcrystalline solid. Single crystal X-ray diffraction of **4** revealed a metal rearrangement, hence the silver ions of the metal precursor displaced the gold atoms in the amidinate pocket of compound **2**, while the gold ions are consecutively coordinated by the acetylide moieties and the phosphines (Figure 3, right).

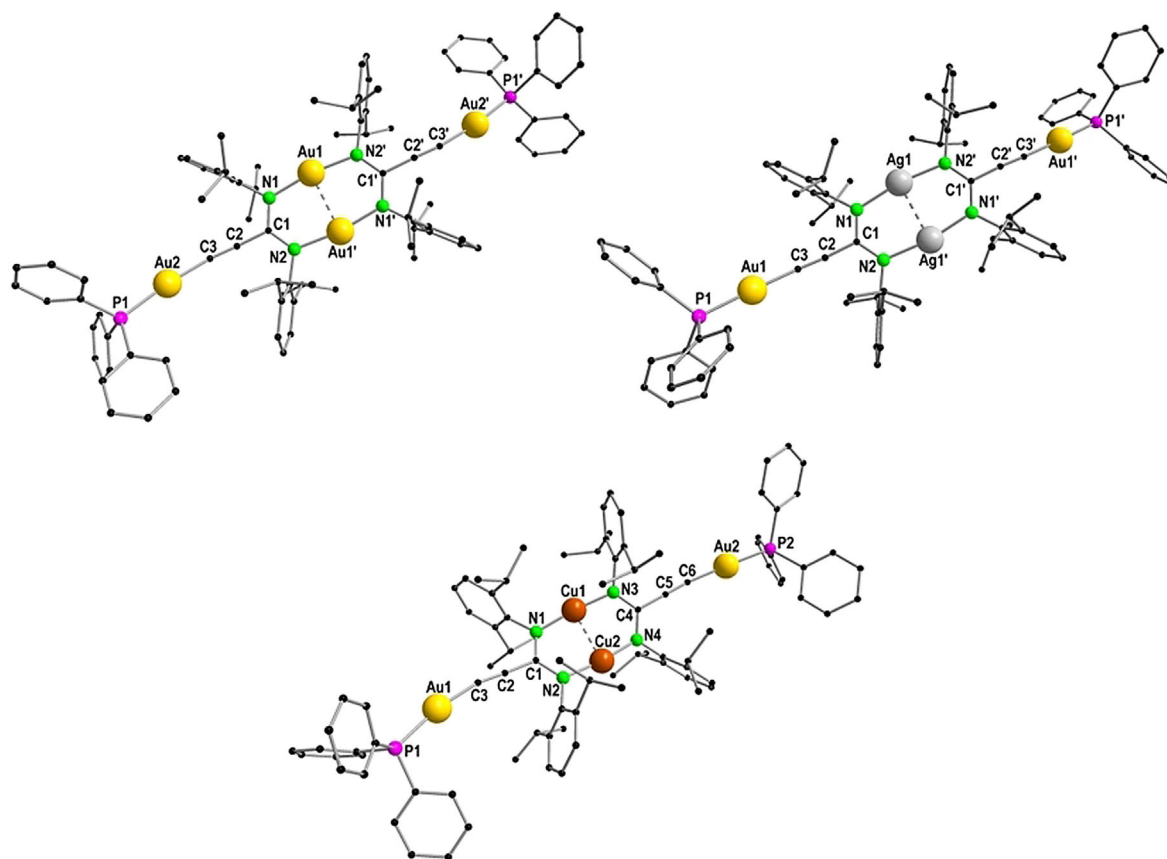


Figure 3. Molecular structures of compounds **3** (left), **4** (right), and **7** (below) in the solid state. Hydrogen atoms are omitted for clarity. Structural parameters are given in the Supporting Information.

The metal–metal contact (Ag1–Ag1' 2.7042(5) Å) in compound **4** is nearly identical to the contact in compound **3** (Au1–Au1' 2.7040(5) Å). The Au1–P1 (2.2767(10) Å) and Au1–C3 (2.006(4) Å) distances, as well as the C3–Au1–P1 (176.26(11)°) angles are also in the same range as for complex **3**.

The ^1H , $^{13}\text{C}\{^1\text{H}\}$, as well as the $^{31}\text{P}\{^1\text{H}\}$ NMR spectra of the silver complex are very similar to the spectra of compound **3**, which partly is a result of the metal rearrangement. The stretching mode of the alkyne moieties is also quite similar and appears at $\tilde{\nu}(\text{C}\equiv\text{C})=2109\text{ cm}^{-1}$ in the IR and Raman spectra of **4**.

In order to complete the series of the tetranuclear coinage metal complexes, we synthesized the digold–dicopper complex $[\{(\text{PPh}_3)\text{Au}\equiv\text{CC}(\text{NDipp})_2\}_2\text{Cu}_2]$ (**7**), with two copper atoms in the central amidinate pocket (Scheme 1). Since a metal rearrangement of copper and gold, as observed for the access of **4**, is not possible, a route similar to the synthesis of **3** was chosen. Therefore, the dicopper complex $[\{\text{Me}_3\text{SiC}\equiv\text{CC}(\text{NDipp})_2\}_2\text{Cu}_2]$ (**5**) was synthesized in a similar fashion as $[\{\text{Me}_3\text{SiC}\equiv\text{CC}(\text{NDipp})_2\}_2\text{Au}_2]$, and was consecutively desilylated to yield $[\{\text{HC}\equiv\text{CC}(\text{NDipp})_2\}_2\text{Cu}_2]$ (**6**). Due to the occurrence of side reactions during the deprotection with CsF, the desilylation was realized using potassium carbonate to obtain compound **6** in nearly quantitative yield and high purity. *In situ* lithiation and subsequent metathesis reaction with two equivalents of $[\text{AuCl}(\text{PPh}_3)]$ yielded compound **7** in a total yield of

49% over three steps. All copper containing compounds (**5**–**7**) have been fully characterized including HR-ESI mass spectrometry and single crystal X-ray diffraction.

The NMR spectra for compound **5** are in full agreement with the measured spectra for $[\{\text{Me}_3\text{SiC}\equiv\text{CC}(\text{NDipp})_2\}_2\text{Au}_2]$, for example, the alkyne moiety in the $^{13}\text{C}\{^1\text{H}\}$ NMR spectrum is detected at similar resonances ($\delta=105.6$ and 95.3 ppm (**5**) vs. $\delta=109$ and 97.3 ppm). Also in consistence, no $\tilde{\nu}(\text{C}\equiv\text{C})$ vibration is observed in the IR spectrum, while it appears as the vibration mode with the highest intensity in the Raman spectrum of **5** at similar wavenumbers ($\tilde{\nu}(\text{C}\equiv\text{C})=2162\text{ cm}^{-1}$ (**5**) vs. $\tilde{\nu}(\text{C}\equiv\text{C})=2167\text{ cm}^{-1}$ in $[\{\text{Me}_3\text{SiC}\equiv\text{CC}(\text{NDipp})_2\}_2\text{Au}_2]$). The molecular structure of **5** in the solid state (Figure S39) shows, in agreement with the smaller ionic radius of the copper(I) ion, an even shorter metal–metal contact (Cu1–Cu2 2.4573(7) Å) than for $[\{\text{Me}_3\text{SiC}\equiv\text{CC}(\text{NDipp})_2\}_2\text{Au}_2]$ (Au1–Au1' 2.7009(11) Å), which is in the usual range for cuprophilic interactions.^[21]

In analogy to the desilylated gold(I) complex **1**, a separate singlet resonance at $\delta(\text{C}_6\text{D}_6)=1.79$ ppm is detected in the ^1H NMR spectrum of **6**, which can be assigned to the terminal alkyne protons. In comparison to the resonance in the ^1H NMR spectrum of **1** ($\delta(\text{CDCl}_3)=2.64$ ppm), it is significantly shifted to higher ppm values which likely results from the less polar solvent C_6D_6 . In good agreement with the previously discussed results, a similar shift of the alkyne carbon atoms ($\delta=87$ and

74.8 ppm) is observed in the $^{13}\text{C}\{^1\text{H}\}$ NMR spectrum of **6** in comparison to the spectrum of **5**.

Furthermore, the two characteristic bands for the stretching modes of the terminal alkyne at $\tilde{\nu}(\text{C}-\text{H}) = 3267\text{ cm}^{-1}$ and $\tilde{\nu}(\text{C}\equiv\text{C}) = 2109\text{ cm}^{-1}$ arise in the IR spectrum of **6** as well.

Compared to **5**, the band of the alkyne stretching mode $\tilde{\nu}(\text{C}\equiv\text{C})$ at 2107 cm^{-1} in the Raman spectrum of **6** is shifted by about 55 cm^{-1} to smaller wavenumbers. This is in agreement with the observations on the analogue gold(I) complexes (shift = 53 cm^{-1}). A metal–metal contact ($\text{Cu1}-\text{Cu1}'$ $2.5319(12)\text{ \AA}$), which is comparable to the value for **5** is observed. All other central structural parameters in the molecular structure of **6** in the solid state solely show small deviations as well.

Moreover, the spectroscopic data for **7** is also in full agreement with the corresponding gold(I) and silver(I) complexes **3** and **4**. Thus, the ^1H NMR spectrum of **7** shows the characteristic separate multiplet in the range of $\delta = 7.50\text{--}7.28\text{ ppm}$ for the aromatic phosphine protons, while a singlet resonance is observed in the $^{31}\text{P}\{^1\text{H}\}$ NMR spectrum ($\delta = 41.5\text{ ppm}$). This resonance is in the range of **3** and **4**.

The molecular structure of compound **7** reveals a metal–metal contact of $\text{Cu1}-\text{Cu2}$ $2.4717(12)\text{ \AA}$, which is nearly the same as for complex **5**. Thus, alterations at the terminal alkyne function do not significantly influence the central M_2 core.

Photoluminescence properties

Compounds **1–7** are either colorless or off-white solids. All of them show azure, bright blue or blue-green photoluminescence (PL) both at low and ambient temperatures, with a moderate rise of PL intensity by decreasing the temperature from 295 to 20 K (Figures 4 and 5, see also the SI). The emission spectra show a similar vibronic structure, particularly distinct at low temperatures and for complex **4**. In consistency with colorlessness, the PL excitation (PLE) spectra of **1–7** show the absorption onset below approximately 450 nm. The PL decay of **1–7** (upon nsec-pulsed excitation with a nitrogen laser at 337 nm) occurs on a microsecond time scale, thus clearly indicating that the PL is phosphorescence (Figure S53). The PL lifetimes decrease moderately upon raising the temperature to 295 K, thus roughly correlating with the decrease of PL intensity due to enhanced nonradiative relaxation. Figure 4 combines PL spectra of the binuclear metal complexes **1**, **5**, and **6**. The blue-green emission of the silylated copper-complex **5** is centered at approximately 520 nm and is similar to that of the gold-complex $[\{\text{Me}_3\text{SiC}\equiv\text{CC}(\text{NDipp})_2\}_2\text{Au}_2]$.^[15] In comparison, the PL emission and excitation spectra of the desilylated compounds **1** and **6** are blue-shifted by approximately 20 nm. In difference to **5**, the reduction of PL intensity of **1** and **6** is more pronounced upon raising the temperature from 20 to 295 K. Correspondingly, PL quantum yields $\varphi(295\text{ K}) = 34$, 16 and 10% were determined using an integrating sphere under ambient conditions for compounds **1**, **5**, and **6**, respectively. There are also some differences in the PL decay. While it is monoexponential for **1** and **5**, with lifetimes $\tau = 56$ (24) and 220 (173) μsec at 20 K (295 K), respectively, the PL decay curve

of **6** transforms from monoexponential at 20 K ($\tau = 252\text{ }\mu\text{sec}$) to biexponential at ambient temperature (Figure S53).

Figure 5 shows the spectra of the tetranuclear complexes **2–4** and **7**. All these complexes emit in the blue color region with the PL bands centered at approximately 450–490 nm. Hence, the PL of the tetranuclear metal complexes is blue-shifted in comparison to the dinuclear metal complexes **1**, **5**, and **6** by approx. 40 nm. At 20 K, a similar vibronic structure of the emissions, comparable to compounds **1**, **5**, and **6**, is observed for **2**, **3**, and **7**.

Likely due to a higher sample crystallinity, **4** exhibits particularly sharp vibronic features under cryogenic conditions, assigned to vibrational modes at approx. 1380 cm^{-1} (probably a bisamidinate-based mode) and 2100 cm^{-1} ($\text{C}\equiv\text{C}$ stretching) and their overtones (Figure S54). Upon raising the temperature from 20 to 295 K, the PL intensity decreases nearly linearly for

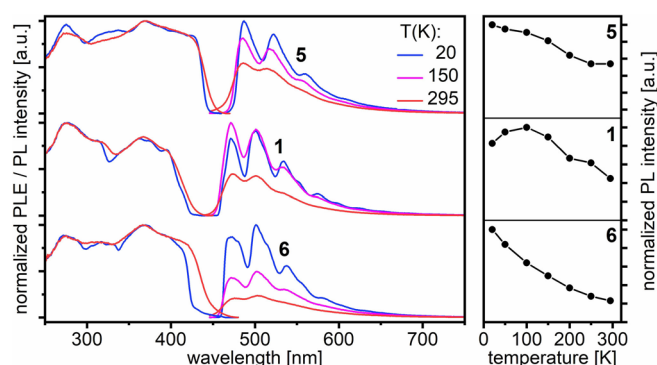


Figure 4. Left: normalized photoluminescence excitation (PLE) and emission (PL) spectra of the binuclear compounds **5**, **1**, and **6** at 20, 150, and 295 K. The PL/PLE spectra were excited/recorded at values between 350–370/407–502 nm, respectively (Table S3). Right: integrated PL intensities vs. temperature in the range of 20 to 295 K.

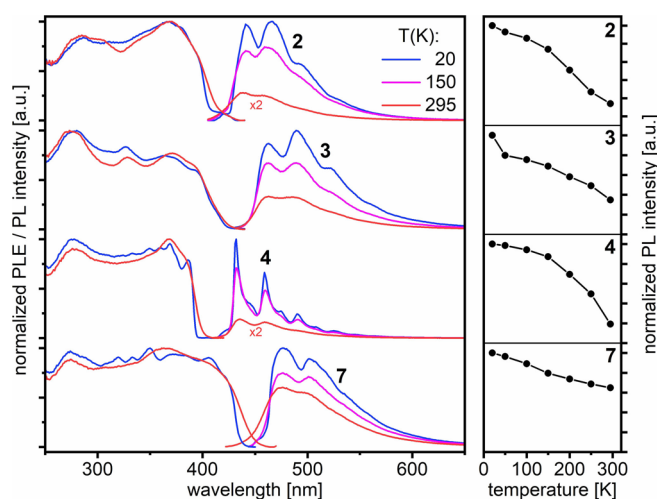


Figure 5. Left: normalized photoluminescence excitation (PLE) and emission (PL) spectra of the tetranuclear compounds **2**, **3**, **4**, and **7** at 20, 150, and 295 K. The PL/PLE spectra were excited/recorded at values between 350–365/432–476 nm, respectively (Table S4). The PL spectral intensities of compounds **2** and **4** at 295 K were multiplied by a factor of 2 for clarity. Right: integrated PL intensities vs. temperature in the range of 20 to 295 K.

all tetranuclear complexes (Figure 5, right). The decrease is quite moderate for gold-gold and gold-copper compounds **3** and **7** and more pronounced for lithium-gold and gold-silver compounds **2** and **4**. In line with this observation, the highest quantum yields $\varphi(295\text{ K}) = 40$ and 41% were found for **3** and **7**, in comparison with 13 and 18% for **2** and **4**, respectively, by using an integrating sphere and excitation at 350 nm (Table S4). The time scale of emission decay of the tetranuclear complexes, e.g., tens to hundreds of microseconds at 20 K is comparable to the binuclear compounds. However, the decay kinetics of the former is more complicated and follows biexponential curves both at low and ambient temperatures (Figure S53). The similarity of the PL properties of compounds **1–7** suggest common types of the emissive triplet excited states. These are likely mostly located on the Dipp-amidinate-alkynyl framework and moderately affected by variation of the coinage metals and coordination patterns across **1–7**.

For instance, the structurally closely related bi- and tetranuclear gold complexes **1** and **3** demonstrate quite similar PL properties, indicating a moderate effect of the gold atoms linearly coordinated by the acetylide moieties. On the other hand, the metals in the central amidinate pocket apparently affect the triplet (non)radiative relaxation rates: as expected for more efficient spin-orbit coupling associated with the gold atoms, the PL decay of **1** and **3** is notably faster in comparison to their copper-containing counterpart structures **6** and **7** (Figure S53). To further determine and compare the specific colors emitted by compounds **1–7**, CIE coordinate diagrams at 295 K (Figure 6) and 20 K (Figure S55) were prepared.^[22] The bimetallic compounds **1**, **5**, and **6** clearly emit in the cyan-green color range, while the PL colors of the tetrametallic complexes **3** and **7** are further shifted to the blue color range. Remarkably azure blue colored PL is observed for the Li_2Au_2 and Ag_2Au_2 complexes **2** and **4**, respectively. At cryogenic temperatures, the emission colors are only slightly shifted (Figure S55).

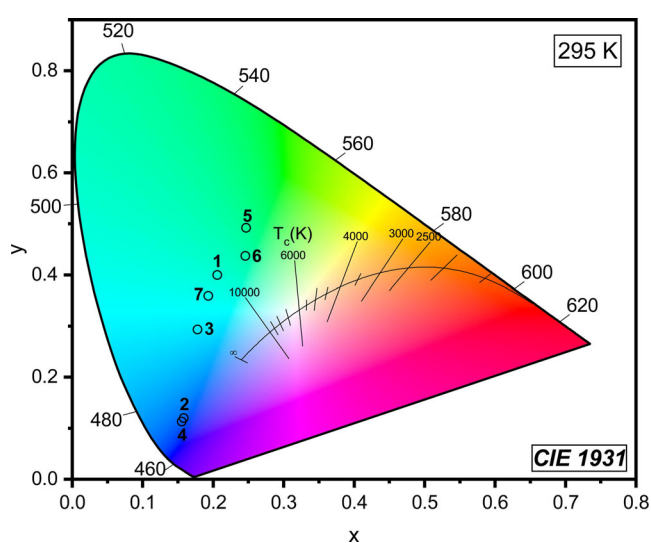


Figure 6. CIE 1931 graph for compounds **1–7** at 295 K . A graph at 20 K can be found in the supporting information (Figure S55).

Since complexes **3** and **7** show the highest PL quantum yields in the solid state, we further investigated their PL properties in thf solution. The observed emission spectra are quite similar to those in the solid state (Figures S49–S51). The PLE spectra well correspond to the respective absorption spectra in solution and qualitatively correspond to the PLE spectra in the solid state. Note that in the latter spectra weak absorption features appear overemphasized due to non-validity of Lambert–Beer law for the optically “thick” solid sample preparations. Finally, PL quantum yields of 15% were measured for both complexes in thf solution.

Conclusions

A straightforward synthetic protocol towards a full series of tetrametallic coinage metal acetylide-amidinate complexes $[(\text{PPh}_3)_2\text{AuC}\equiv\text{CC}(\text{NDipp})_2]_2\text{M}_2$ ($\text{M} = \text{Cu}, \text{Ag}, \text{Au}$) is presented. We demonstrated that the ethynyl compound $[\text{HC}\equiv\text{CC}(\text{NDipp})_2]_2\text{M}_2$ ($\text{M} = \text{Cu}, \text{Au}$) serves as a versatile metalloligand. The gold compound even undergoes ligand exchange reactions when treated with silver precursors. The obtained metal complexes exhibit a combination of a very short intrinsic fully supported metallophilic interaction and two gold(I)triphenylphosphine moieties which are linearly aligned towards each other.

All metal complexes emit azure, bright blue or blue-green phosphorescence with quantum yields of up to 41% in the solid state under ambient conditions. Furthermore, a similar and efficient PL with quantum yields of 15% was observed for two exemplary complexes when dissolved in thf. Similar properties have also been observed for the previously characterized alkynyl substituted gold(I) amidinate and its octanuclear derivative.^[15] Accordingly, the efficient PL, both in the solid state and in solution, appears to be a characteristic feature of the dimeric coinage metal amidinate structural motif.

Experimental Section

Experimental details are given in the Supporting Information (SI) which is available free of charge via the internet. The Supporting Information includes Materials, characterization methods, experimental procedures, full spectroscopic data for all new compounds, copies of ^1H , $^{13}\text{C}\{^1\text{H}\}$, $^{31}\text{P}\{^1\text{H}\}$, $^7\text{Li}\{^1\text{H}\}$ NMR, IR and Raman spectra, elemental analyses, crystallographic data, additional photoluminescence and UV/Vis spectra.

Acknowledgements

Financial support by the DFG-funded transregional collaborative research center SFB/TRR 88 “Cooperative Effects in Homo and Heterometallic Complexes (3MET)” is gratefully acknowledged (projects C3 and C7). We thank Prof. Dr. Christopher Barner-Kowollik from the Queensland University of Technology (QUT) for his support regarding the mass spectrometry measurements. Open access funding enabled and organized by Projekt DEAL.

Conflict of interest

The authors declare no conflict of interest.

Keywords: acetylide · amidinate · desilylation · gold · luminescence

- [1] J. M. López-de-Luzuriaga, M. Monge, M. E. Olmos, *Dalton Trans.* **2017**, 46, 2046–2067.
- [2] C.-M. Che, S.-W. Lai, *Coord. Chem. Rev.* **2005**, 249, 1296–1309.
- [3] a) P. Ai, A. A. Danopoulos, P. Braunstein, K. Y. Monakhov, *Chem. Commun.* **2014**, 50, 103–105; b) S. Bestgen, M. T. Gamer, S. Lebedkin, M. M. Kappes, P. W. Roesky, *Chem. Eur. J.* **2015**, 21, 601–614; c) R. Zhong, A. Pöthig, D. C. Mayer, C. Jandl, P. J. Altmann, W. A. Herrmann, F. E. Kühn, *Organometallics* **2015**, 34, 2573–2579; d) C. Kiefer, S. Bestgen, M. T. Gamer, M. Kühn, S. Lebedkin, F. Weigend, M. M. Kappes, P. W. Roesky, *Chem. Eur. J.* **2017**, 23, 1591–1603; e) T. Simler, P. Braunstein, A. A. Danopoulos, *Dalton Trans.* **2016**, 45, 5122–5139.
- [4] a) W.-H. Chan, S.-M. Peng, C.-M. Che, *J. Chem. Soc. Dalton Trans.* **1998**, 2867–2872; b) M. K. Penney, R. Giang, K. K. Klausmeyer, *Polyhedron* **2015**, 34, 275–283; c) X.-L. Chen, R. Yu, X.-Y. Wu, D. Liang, J.-H. Jia, C.-Z. Lu, *Chem. Commun.* **2016**, 52, 6288–6291.
- [5] J. Carlos Lima, L. Rodríguez, *Chem. Soc. Rev.* **2011**, 40, 5442–5456.
- [6] T. P. Seifert, N. D. Knoefel, T. J. Feuerstein, K. Reiter, S. Lebedkin, M. T. Gamer, A. C. Boukis, F. Weigend, M. M. Kappes, P. W. Roesky, *Chem. Eur. J.* **2019**, 25, 3799–3808.
- [7] A. K. Gupta, A. Orthaber, *Chem. Eur. J.* **2018**, 24, 7536–7559.
- [8] a) V. Wing-Wah Yam, E. Chung-Chin Cheng, *Photochemistry and Photophysics of Coordination Compounds II*, Vol. 281 (Eds.: V. Balzani, S. Campagna), Springer, Heidelberg, **2007**, pp. 269–309; b) E. V. Grachova, *Russ. J. Gen. Chem.* **2019**, 89, 1102–1114.
- [9] a) S. Sculfort, P. Braunstein, *Chem. Soc. Rev.* **2011**, 40, 2741–2760; b) C.-M. Che, H.-Y. Chao, V. M. Miskowski, Y. Li, K.-K. Cheung, *J. Am. Chem. Soc.* **2001**, 123, 4985–4991; c) W. Lu, H.-F. Xiang, N. Zhu, C.-M. Che, *Organometallics* **2002**, 21, 2343–2346; d) T. E. Müller, S. W.-K. Choi, D. M. P. Mingos, D. Murphy, D. J. Williams, V. Wing-Wah Yam, *J. Organomet. Chem.* **1994**, 484, 209–224; e) V. Wing-Wah Yam, K. Kam-Wing Lo, *Chem. Soc. Rev.* **1999**, 28, 323–334; f) H. Schmidbaur, A. Schier, *Chem. Soc. Rev.* **2008**, 37, 1931–1951; g) V. W.-W. Yam, E. C.-C. Cheng, *Chem. Soc. Rev.* **2008**, 37, 1806–1813; h) H. Schmidbaur, A. Schier, *Angew. Chem. Int. Ed.* **2015**, 54, 746–784; *Angew. Chem.* **2015**, 127, 756–797.
- [10] a) V. W.-W. Yam, C.-L. Chan, C.-K. Li, K. M.-C. Wong, *Coord. Chem. Rev.* **2001**, 216–217, 173–194; b) M. A. Omary, A. A. Mohamed, M. A. Rawashdeh-Omary, J. P. Fackler, *Coord. Chem. Rev.* **2005**, 249, 1372–1381.
- [11] E. Andris, P. C. Andrikopoulos, J. Schulz, J. Turek, A. Růžička, J. Roithová, L. Rulišek, *J. Am. Chem. Soc.* **2018**, 140, 2316–2325.
- [12] H. Schmidbaur, A. Schier, *Chem. Soc. Rev.* **2012**, 41, 370–412.
- [13] D. Fenske, G. Baum, A. Zinn, K. Dehnicke, *Z. Naturforsch. B* **1990**, 45, 1273.
- [14] a) H. E. Abdou, A. A. Mohamed, J. P. Fackler, *Inorg. Chem.* **2005**, 44, 166–168; b) H. E. Abdou, A. A. Mohamed, J. P. Fackler, *Inorg. Chem.* **2007**, 46, 141–146; c) H. E. Abdou, A. A. Mohamed, J. P. Fackler, *J. Cluster Sci. Coord. Chem. Rev.* **2010**, 254, 1253–1259; e) T. Seifert, V. R. Naina, T. J. Feuerstein, N. D. Knoefel, P. W. Roesky, *Nanoscale* **2020**, 12, <https://doi.org/10.1039/d0nr04748a>; f) F. T. Edelmann, *Adv. Organomet. Chem. Vol. 61* (Eds.: F. H. Anthony, J. F. Mark), Academic Press, **2013**, pp. 55–374.
- [15] T. J. Feuerstein, M. Poß, T. P. Seifert, S. Bestgen, C. Feldmann, P. W. Roesky, *Chem. Commun.* **2017**, 53, 9012–9015.
- [16] T. J. Feuerstein, Synthese photolumineszenter Metallkomplexe, UV-LED-NMR-Charakterisierung eines photolabilen Komplexes sowie photolithographische Immobilisierung von Metallopolymeren, PhD Thesis, Karlsruhe Institute of Technology (KIT), Karlsruhe, Germany, **2019**.
- [17] a) A. C. Jones, A. W. Sanders, M. J. Bevan, H. J. Reich, *J. Am. Chem. Soc.* **2007**, 129, 3492–3493; b) C. Citek, P. H. Oyala, J. C. Peters, *J. Am. Chem. Soc.* **2019**, 141, 15211–15221.
- [18] W. J. Evans, D. K. Drummond, T. P. Hanusa, J. M. Olofson, *J. Organomet. Chem.* **1989**, 376, 311–320.
- [19] a) J. Vicente, M.-T. Chicote, M.-D. Abrisqueta, P. G. Jones, *Organometallics* **1997**, 16, 5628–5636; b) G. F. Manbeck, M. C. Kohler, M. R. Porter, R. A. Stockland, Jr., *Dalton Trans.* **2011**, 40, 12595–12606; c) M. Pérez-Iglesias, P. Espinet, J. A. Casares, *Inorg. Chem.* **2018**, 57, 11193–11200.
- [20] a) J. Vicente, M.-T. Chicote, M. M. Alvarez-Falcón, P. G. Jones, *Organometallics* **2005**, 24, 5956–5963; b) M. Lohan, P. Ecorchard, T. Ruffer, F. Justaud, C. Lapinte, H. Lang, *Organometallics* **2009**, 28, 1878–1890; c) R. Zhang, C. Zhao, X. Li, Z. Zhang, X. Ai, H. Chen, R. Cao, *Dalton Trans.* **2016**, 45, 12772–12778.
- [21] N. V. S. Harisomayajula, B.-H. Wu, D.-Y. Lu, T.-S. Kuo, I.-C. Chen, Y.-C. Tsai, *Angew. Chem. Int. Ed.* **2018**, 57, 9925–9929; *Angew. Chem.* **2018**, 130, 10073–10077.
- [22] Chromaticity Diagram add-on for OriginPro 2018b (64-bit), Copyright (c) 1991–2018 OriginLab Corporation.

Manuscript received: May 19, 2020

Accepted manuscript online: June 10, 2020

Version of record online: ■■■■■ 0000

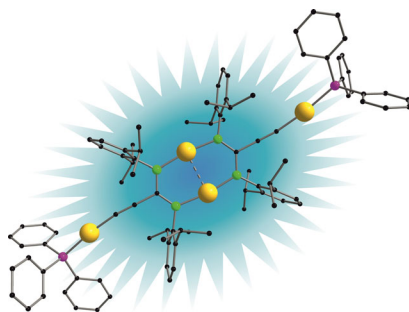
FULL PAPER

Synthesis Design

 T. J. Feuerstein, T. P. Seifert, A. P. Jung,
R. Müller, S. Lebedkin, M. M. Kappes,
P. W. Roesky*

■■ - ■■

  **Efficient Blue Phosphorescence in
Gold(I)-Acetylide Functionalized
Coinage Metal Bis(amidinate)
Complexes**



Two plus two is four: The synthesis of linear symmetric ethynyl- and acetylide-amidinates of the coinage metals is presented. Their photophysical properties were thoroughly investigated in a temperature range of 20–295 K. Short lifetimes and quantum yields of up to 41 % were determined. Furthermore, the complexes show pronounced PL in thf solution as well.